Influence of palmitic acid and hexadecanol on the phase transition temperature and molecular packing of dipalmitoylphosphatidyl-choline monolayers at the air–water interface

Ka Yee C. Lee[a] and Ajaykumar Gopal
Department of Chemistry & Institute for Biophysical Dynamics, The University of Chicago, Chicago, Illinois 60637

Anja von Nahmen and Joseph A. Zasadzinski
Department of Chemical Engineering, University of California, Santa Barbara, California 93106-5080

Jaroslaw Majewski and Gregory S. Smith
Manuel Lujan Jr. Neutron Scattering Center, LANSCE-12, Los Alamos National Laboratory, Los Alamos, New Mexico 87545

Paul B. Howes and Kristian Kjaer
Department of Solid State Physics, Risø National Laboratory, DK-4000, Roskilde, Denmark

(Received 3 July 2001; accepted 2 October 2001)

Palmitic acid (PA) and 1-hexadecanol (HD) strongly affect the phase transition temperature and molecular packing of dipalmitoylphosphatidylcholine (DPPC) monolayers at the air–water interface. The phase behavior and morphology of mixed DPPC/PA as well as DPPC/HD monolayers were determined by pressure-area-isotherms and fluorescence microscopy. The molecular organization was probed by synchrotron grazing incidence x-ray diffraction using a liquid surface diffractometer. Addition of PA or HD to DPPC monolayers increases the temperature of the liquid-expanded to condensed phase transition. X-ray diffraction shows that DPPC forms mixed crystals both with PA and HD over a wide range of mixing ratios. At a surface pressure (π) of 40 mN/m, increasing the amount of the single chain surfactant leads to a reduction in tilt angle of the aliphatic chains from nearly 30° for pure DPPC to almost 0° in a 1:1 molar ratio of DPPC and PA or HD. At this composition we also find closest packing of the aliphatic chains. Further increase of the amount of PA or HD does not change the lattice or the tilt. © *2002 American Institute of Physics.* [DOI: 10.1063/1.1420730]

I. INTRODUCTION

Biological membranes encapsulate the contents of every cell and organelle, thereby isolating the inner compartment from the outer media. A variety of important processes take place at the membrane interface. For most of these processes, the fluidity of the membrane is a crucial factor. For example, the permeability of small ions such as Na^+ is greatest close to the main phase transition.[1] Pancreatic phospholipase A_2 selectively binds to gel-phase lipids, but is only enzymatically active in the hydrolysis of lipids in the fluid phase.[2] Changes in the lipid fluidity are also associated with morphological changes in the bilayer.[3,4] Membrane fluidity can be increased either by increasing the degree of lipid unsaturation or by decreasing the length of the acyl chains.[5] Peptides and other small molecules can shift the phase transition temperature. The addition of small amounts of short chain fatty acids and *n*-alcohols to phospholipid membranes results in higher fluidity.[3,6,7] Larger concentrations of short chain alcohols induce an interdigitation of the two monolayers within the bilayer and a decrease in fluidity.[8] Long chain fatty acids and *n*-alcohols increase the phase transition temperature of DPPC[6,9–11] and disaturated phosphatidylserines.[12]

We find that fatty acids and *n*-alcohols alter the phase behavior of DPPC monolayers at the air–water interface, which has important implications for biophysical properties of natural and replacement lung surfactants.[13–16] Lung surfactant (LS) is a two-dimensional (2D) complex mixture of lipids and proteins that lines the surface of lung alveoli.[16,17] LS contains a number of lipids and specific proteins; the predominant lipid (40–50% by weight) is the saturated phospholipid dipalmitoylphosphatidylcholine (DPPC).[16–18] *In vitro* studies show that palmitic acid (PA), which is a minor fraction (5–10% by weight) of natural LS and a common additive to replacement lung surfactants, improves the surface properties of synthetic lung surfactants.[14,15,19,20] PA, or its corresponding alcohol, 1-hexadecanol (HD), in combination with DPPC and various anionic lipids has been used as a lipid matrix in replacement surfactants to treat Respiratory Distress Syndrome.[13,15,19,21]

However, the function of PA in natural lung surfactants is not particularly well understood.[14] In addition, there is, as yet, no general agreement on the appropriate fraction of PA or HD in replacement surfactants,[13–15,17] although these lipids are added to supplement both animal extract based and synthetic lung surfactants. To address these questions, the phase behavior and morphology of mixed DPPC/PA and DPPC/HD monolayers were determined by pressure-area-

[a]Author to whom correspondence should be addressed.

isotherms and fluorescence microscopy. The in-plane molecular organization was probed by synchrotron grazing incidence x-ray diffraction (GIXD) using a liquid surface diffractometer. We find that both PA and HD strongly affect the phase transition temperatures and molecular organization of DPPC monolayers. Addition of PA or HD to DPPC increases the temperature of the liquid-expanded to condensed phase transition; that is, adding PA or HD is roughly equivalent to lowering the temperature of a pure DPPC monolayer. X-ray diffraction shows that DPPC forms mixed crystals (the components do not phase separate) both with PA and HD over a wide range of mixing ratios. For the surface pressure of 40 mN/m, increasing the amount of PA or HD leads to a reduction in tilt angle of the aliphatic chains from $\approx 30°$ for pure DPPC to near 0° at a 1:1 molar ratio of DPPC and PA or HD. At this composition we also find the closest packing of the aliphatic chains. Further increase of the amount of PA or HD does not change the lattice or the tilt. The coherence length of the packing, an indication of the extent of ordering, also increases with increasing PA or HD content. These results show that the concentrations of PA and HD found in natural and replacement lung surfactants make the DPPC monolayer better ordered, and effectively make the monolayer more rigid. At 40 mN/m, PA and HD are localized almost exclusively in the condensed phase domains of the LS monolayer. The changes induced in the solid phase of the monolayer, in turn, likely alter its collapse and respreading behavior.[22] PA appears to be necessary to adjust the solid phase properties in natural lung surfactants, which helps to explain the need for PA or HD in replacement lung surfactants.

II. MATERIALS AND METHODS

A. Materials

1,2-dipalmitoyl-sn-glycero-3-phosphocholine (DPPC) was purchased from Avanti Polar-Lipids (Alabaster, AL) and used without further purification. Palmitic acid (99%) was obtained from Aldrich Chemical (Milwaukee, MO) and 1-hexadecanol (>99%) from Fluka (Milwaukee, MO).

B. Methods

Surface pressure-area (Langmuir) isotherms and fluorescence microscopy (FM) images were obtained with a home-built Langmuir trough with an attached fluorescence microscope (FM).[23] Surfactants were dissolved in chloroform (HPLC grade, Fluka, Milwaukee, MO), mixed in the desired ratios, and deposited at the air–water interface of the trough with a microsyringe. To develop contrast in the FM images, 0.5 mol % of the lipid-analog fluorescent dye, 4,4-difluoro-5, 7- dimethyl-4- bora-3a, 4a-diaza-s-indacene-3-dodecanoic acid (BODIPY® FL C_{12}, $\lambda_{505/511}$ and $\varepsilon = 87\,000$), from Molecular Probes (Eugene, OR) was used. The dye preferentially segregates to the less ordered regions of the monolayer and appears bright in the images.[24–27] All experiments were performed on a pure water subphase of 18.2 MΩ Millipore water obtained from a Milli-Q UV Plus system (Millipore, Bedford, MA) at 30 °C. The solvent was allowed to evaporate for at least 15 min prior to beginning any isotherm. The compression rate was 0.1 mm/s.

All synchrotron x-ray measurements were carried out using the liquid surface diffractometer at the BW1 (undulator) beam line at HASYLAB, DESY (Hamburg, Germany).[28,29] A temperature-controlled Langmuir trough, equipped with a Wilhelmy balance for surface pressure measurements, and barriers for surface pressure controls, was mounted on the diffractometer. In a typical experiment, a monolayer of a given composition was first spread using a microsyringe at the desired temperature. At least 30 min were given for complete solvent evaporation before the two-dimensional film was compressed to the desired surface pressure. The film was then held at this surface pressure throughout the experiment. The trough was enclosed in a sealed, helium-filled canister where the oxygen level was constantly monitored.

The synchrotron x-ray beam was monochromated to a wavelength of $\lambda \approx 1.30$ Å by Laue reflection from a Be (200) single crystal. By tilting the normal to the reflecting planes out of the horizontal plane, the monochromatic beam could be bent down to yield a glancing angle with the horizontal liquid surface. For the GIXD experiments, the x-ray beam was adjusted to strike the surface at an incident angle of $\approx 0.11°$, which corresponds to the vertical momentum transfer vector $Q_z = 0.85\,Q_c$, where $Q_c = 0.021\,76\,\text{Å}^{-1}$ is the critical scattering vector for total external reflection. At this angle the incident wave is totally reflected, while the refracted wave becomes evanescent, traveling along the liquid surface. Such a configuration maximizes surface sensitivity.[30] The dimensions of the incoming x-ray beam footprint on the liquid surface were approximately 5 mm×50 mm.

For the collection of the diffracted intensities we used a one-dimensional position sensitive detector (PSD) with vertical acceptance $0 < q_z < 0.9\,\text{Å}^{-1}$, and its axis along the vertical. In front of the PSD, a Soller collimator was mounted which defined the horizontal resolution of the detector, $\Delta q_{xy} = 0.0075\,\text{Å}^{-1}$. The scattered intensity was measured by scanning over a range of the horizontal scattering vector, $q_{xy} \approx (4\pi/\lambda) \cdot \sin(2\theta_{xy}/2)$, where $2\theta_{xy}$ is the angle between the incident and diffracted beam projected onto the horizontal plane, and λ is the wavelength of the x-ray beam. Such a scan, integrated over the whole window of a position sensitive detector (PSD), yields the *Bragg peaks*. Simultaneously, the scattered intensity recorded in channels along the PSD, but integrated over the scattering vector in the horizontal plane across a Bragg peak, produces q_z-resolved scans called *Bragg rod profiles*.

In three-dimensional (3D) crystals, diffraction only takes place when the scattering vector **Q** coincides with $\{h,k,l\}$ points of the reciprocal 3D lattice, giving rise to Bragg spots (h, k, l are the Miller indices). Strong diffraction from a set of crystal planes with an interplanar spacing d occurs only when the Bragg law is obeyed. In our 2D systems and at surface pressures of interest, DPPC monolayers are a mosaic of 2D crystallites with random orientation about the direction normal to the subphase, and can therefore be described as 2D powders. Due to the lack of restriction on the scattering vec-

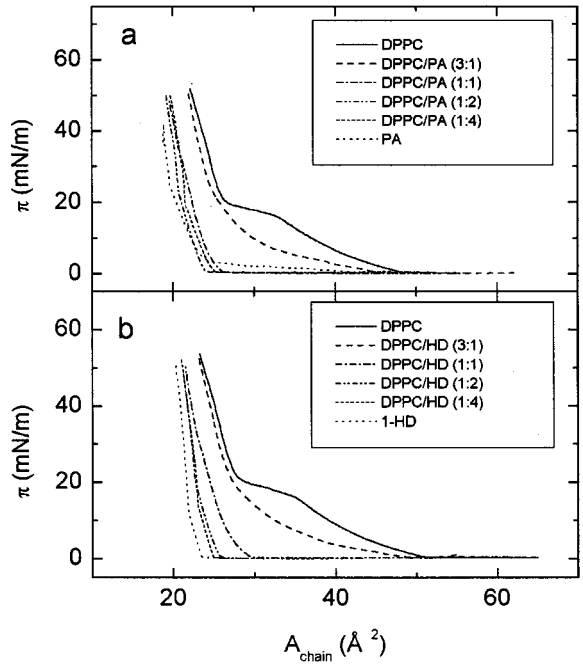

FIG. 1. Isotherms of mixed films of (a) DPPC/PA and (b) DPPC/HD at 30 °C on a water subphase. The area, *A*, is given as area per acyl chain. Each DPPC contributes two acyl chains, and each PA or HD contributes one to the mixture.

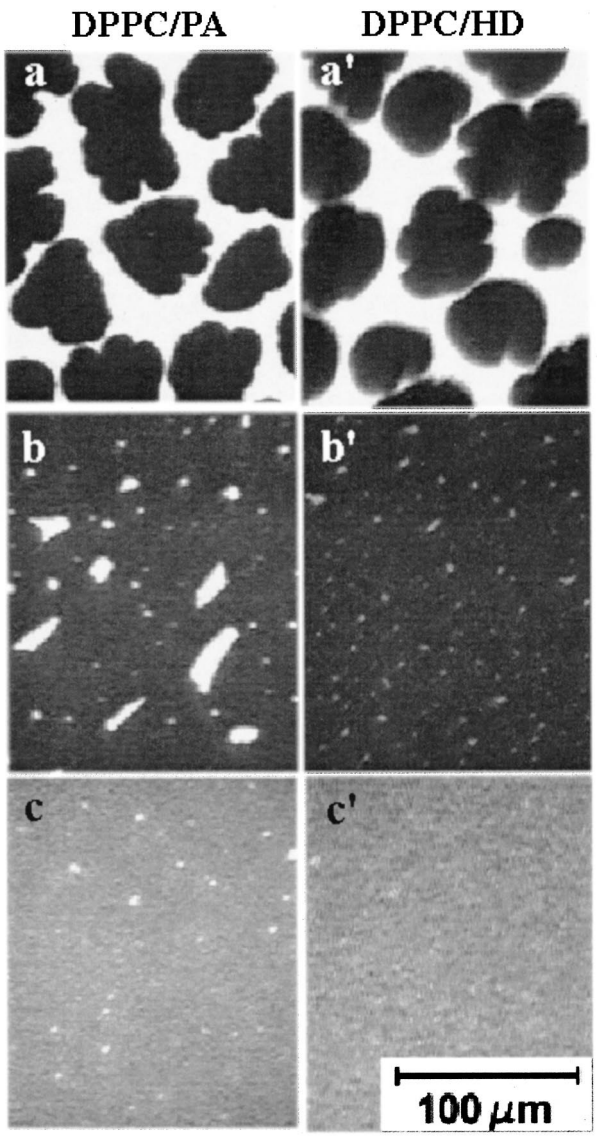

FIG. 2. Fluorescence images of DPPC/PA mixtures with mole ratios (a) 3:1, (b) 1:1, (c) 1:2, and DPPC/HD mixtures with mole ratios (a′) 3:1, (b′) 1:1, (c′) 1:2. Images were obtained using BODIPY® FL C_{12} as fluorescence dye. The BODIPY segregates preferentially into disordered regions of the monolayer, (Ref. 27) rendering liquid-expanded domains bright and condensed regions dark. All images were taken at 30 °C on a water subphase and at a lateral pressure of 15 mN/m. The bright liquid-expanded phase is eliminated with increasing fractions of PA or HD in favor of the dark condensed phase.

tor component Q_z along the direction normal to the crystal, Bragg scattering from a 2D crystal extends as continuous Bragg rods through the reciprocal space.[29,31] The angular positions of the Bragg peaks allow for the determination of the repeat distance *d* for the 2D lattice. From the shapes of the peaks, it is possible to determine the 2D crystalline coherence length, *L* (the average distance in the direction of the reciprocal lattice vector Q_{xy} over which there is ''near-perfect'' crystallinity). The intensity distribution along the Bragg rod can be analyzed to determine the direction and magnitude of the molecular tilt, the out-of-plane coherence length L_c, and the magnitude of molecular motion or surface roughness of the crystallites (Debye–Waller factor).

III. RESULTS

The isotherms of pure DPPC, PA, HD, as well as the DPPC/PA and DPPC/HD mixtures are shown in Fig. 1. 1:1 DPPC/PA stands for an equimolar mixture of DPPC and PA. To simplify the presentation of the isotherms, the ordinate is scaled by the area per hydrocarbon chain (A_{chain}), rather than by the more conventional area per molecule. Each DPPC molecule contributes two chains, and each PA or HD contributes one chain.

At 30 °C on a pure water subphase, pure DPPC undergoes a first order phase transition from a liquid-expanded (*le*) to a condensed (*c*) phase at a surface pressure of about 16 mN/m. This is evident from a pronounced plateau in the isotherm, as well as by the observation of coexisting domains visualized by fluorescence microscopy.[27] A similar first order (*le*–*c*) phase transition is observed for palmitic acid at a pressure of ≈2 mN/m.[26] A second order phase transition (orthorhombic nearest neighbor tilted L_2 phase or next nearest neighbor tilted *Ov* phase to untilted hexagonal *LS* phase[25,32]) is clearly visible as the abrupt change in slope of the isotherm at about 23 mN/m. In contrast, hexadecanol does not show a *le*-*c* phase transition at 30 °C on pure water, and the second order transition (likely from a next nearest neighbor tilted $L_{2'}$ phase to an untilted hexagonal *LS* phase) occurs at 10 mN/m.[25,33,34]

Adding PA or HD to DPPC changes the phase behavior drastically. At a molar ratio of 3:1 of DPPC/PA or DPPC/HD, the isotherm shows a high compressibility region for $\pi < 20$ mN/m (Fig. 1). Fluorescence images show the coexistence of dark and bright domains, indicating that the mixture undergoes a phase transition from a *le* to a *c* phase in that region [Figs. 2(a) and 2(a′)]. In contrast, molar ratios of 1:1, 1:2, 1:4 DPPC/PA or DPPC/HD show no evidence of a *le* phase

even at zero pressure, and hence, are below their respective triple point temperatures[26] at 30 °C. Accordingly, fluorescence images are rather featureless [Figs. 2(b), 2(b′), 2(c), 2(c′)]. At high surface pressure, the isotherms for molar ratios of 1:1 or higher converge to an average area per hydrocarbon chain of about 20 Å^2, as compared to the 26 Å^2 for DPPC in the solid phase. This shows that both PA and HD condense the DPPC lattice. For the 1:2 and 1:4 ratios of DPPC/PA or DPPC/HD, there is a kink in the isotherm at roughly the same surface pressure as either the pure PA or pure HD. This may correspond to the separation of a pure PA or HD phase coexisting with a mixed PA/DPPC or HD/DPPC crystalline phase.

GIXD provides information only on the ordered portions of the monolayer. For diacyl phospholipid monolayers at the air–water interface, diffraction is observed only from the lateral order of the aliphatic chains;[35] the lipid headgroups do not contribute to the diffraction. GIXD experiments were done at surface pressures of 15 mN/m and 40 mN/m. An overview of all the representative Bragg peaks is shown in Fig. 3. The lattice parameters are summarized in Tables I–IV. Note that under the experimental conditions, pure PA is not stable at 40 mN/m (the collapse pressure of PA is about 40 mN/m). Therefore, the Bragg peak for PA shown in Fig. 3(b) was obtained at a lower pressure of 30 mN/m, which is just above the *c* to solid transition. We believe that accounts for the relatively low Q_{xy} value relative to DPPC/PA (1:1, 1:2, 1:4) mixtures.

From our isotherms and fluorescence images, all systems (except for PA) we investigated are in a solid phase at a pressure of 40 mN/m. For solid phase DPPC, we find two Bragg peaks indicating a rectangular unit cell [Figs. 3(b), 3(b′)]. The calculated area per chain of $A=23.3$ Å^2 as well as the tilt angle of 25.5° obtained from Bragg rod analysis (Fig. 4) matches previously published data on DPPC monolayers[36,37] and multilayers;[38] previous results on monolayers at a higher surface pressure of 45 mN/m and a lower temperature of 15 °C gave a smaller tilt angle of 25.0°, which is consistent with our current data. For HD we find only one Bragg peak. The corresponding Bragg rod has its maximum at $Q_z \approx 0$ Å^{-1} (Fig. 4), indicating a hexagonal unit cell with untilted chains and a lattice spacing of 4.82 Å. This finding is also consistent with previously published data on long chain alcohols[25,34,39] (Fig. 4).

For 40 mN/m, a mixed monolayer of DPPC/HD with a molar ratio of 3:1 forms crystals that produce two Bragg peaks indicating a rectangular cell. Detailed analysis of the corresponding Bragg rod profiles [Fig. 4(c)] shows that the aliphatic chains are tilted by 19° (Table IV). Further increase of the HD content leads to a hexagonal unit cell represented by only one Bragg peak [Fig. 3(b′)]. The maximum position of the Bragg peak shifts to higher Q_{xy} values with increasing amounts of HD and approaches the Q_{xy} value obtained with pure HD [Fig. 3(b′)]. As for pure HD, the corresponding Bragg rods have their maximum at $Q_z \approx 0$ Å^{-1} indicating a tilt angle of almost 0° [Fig. 4(b)]. The coherence length of the monolayer also increases with increasing HD content, indicating a better ordered structure. A very similar trend is observed for DPPC/PA mixtures. Results are summarized in

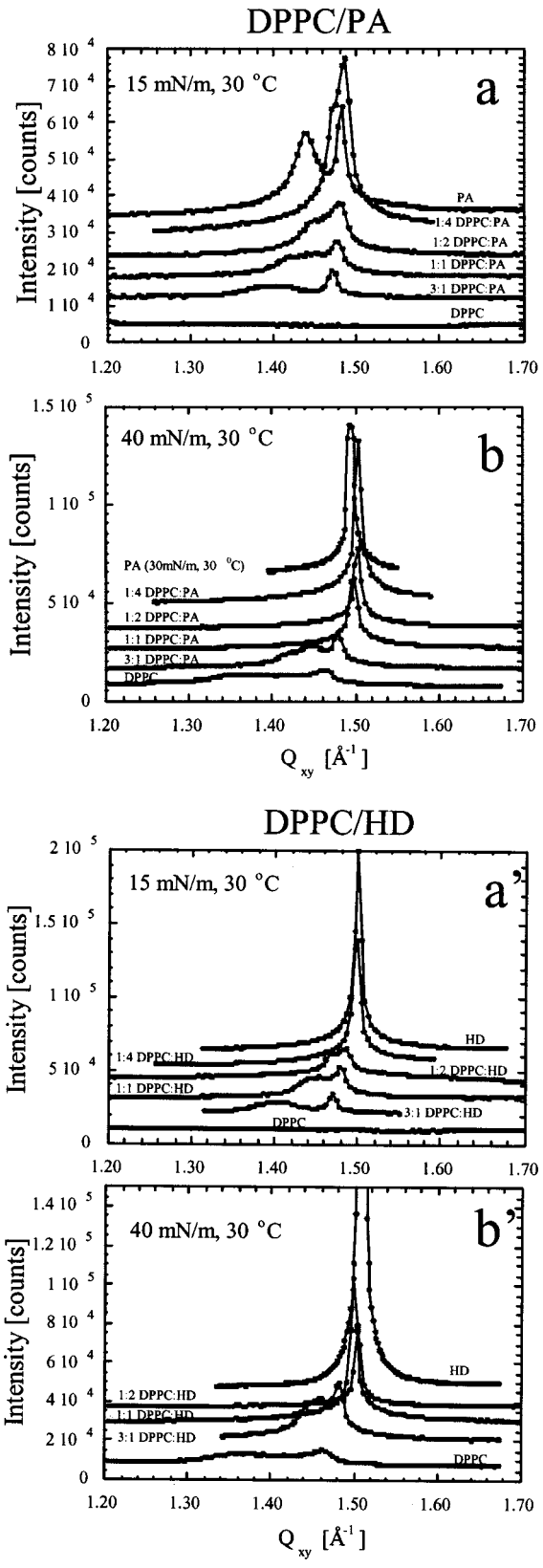

FIG. 3. GIXD data for DPPC/PA mixtures at surface pressures of (a) 15 mN/m and (b) 40 mN/m. (pure PA collapses below 40 mN/m. For comparison, GIXD data were obtained at a pressure of 30 mN/m.) GIXD data for DPPC/PA mixtures at surface pressures of (a′) 15 mN/m and (b′) 40 mN/m. The Bragg peak profiles were obtained by scanning along the horizontal scattering vector Q_{xy} and integrating over the whole Q_z window of the position sensitive detector. For clarity, graphs are shifted along the *y*-axis. All data were obtained at 30 °C. The molecular packing parameters obtained from these data are listed in Tables I–IV.

TABLE I. DPPC:PA mixtures at 15mN/m at 30 °C.

Composition	In-plane Bragg peaks: Observed d-spacing (Å)	Area per chain (Å^2)	Projected area per chain (Å^2)	Unit cell (Å)	Coherence length, L^c (Å)	Out-of-plane Bragg rods: Tilt angle, t (degrees)	Tilt direction (degrees)
DPPC	No in-plane diffraction observed→no in-plane order						
PA	d_{11} 4.37, d_{02} 4.24	21.56	20.07	rectangular $a=5.09$, $b=8.47$	L_{11} 140, L_{02} 560	21.4°	13.2° from NN, non-symmetry
3:1 DPPC:PA	d_{11} 4.49, d_{02} 4.27	22.50	20.31	rectangular[a] $a=5.27$ $b=8.54$	L_{11} 66, L_{02} 540	25.5°	9.8° from NN, non-symmetry
1:1 DPPC:PA	d_{10} 4.22, d_{01} 4.35, d_{11} 4.26	21.79	20.19	oblique[b] $a=5.01$, $b=4.93$ $\gamma=118.1°$	L_{10} 95, L_{01} 250, L_{11} 200	22.1°	15.5° from NN, non-symmetry
1:2 DPPC:PA	d_{11} 4.35, d_{02} 4.26	21.53	20.32	rectangular $a=5.06$ $b=8.51$	L_{11} 105, L_{02} 200	19.3°	17.6° from NN, non-symmetry
1:4 DPPC:PA	d_{11} 4.26, d_{02} 4.23	20.85	19.70	rectangular $a=4.93$ $b=8.47$	L_{11} 150, L_{02} 440	19.1°	18.6° from NN, non-symmetry

[a]Small oblique distortion.
[b]Very close to a rectangular cell: $a=5.10$ Å, $b=8.52$ Å.
[c]$\{hk\}$ denotes a set of Bragg rods (hk) with equal in-plane components $\overline{q}_{xy}^{hk}$, and hence not resolved in GIXD from these 2D powder data. For example, for a hexagonal lattice {10} means {(10),(01)(10)(01)(11)(11)}; for a rectangular lattice {11} means {(11),(11)(11)(11) and {02} means {(02),(02)}. It should be noted that a {centered} rectangular lattice (a_r, $b_r \neq \sqrt{3}a_r$, $\gamma_r=90°$) can also be described as a distorted hexagonal with $a=b$, $\gamma \neq 120°$. The oblique cell is also a distorted hexagonal lattice with $a \neq b$ and $\gamma \neq 120°$.

Table II and Fig. 3(b). Note that even though the Bragg peak of pure PA ($\pi=30$ mN/m) is at lower Q_{xy} value than the corresponding Bragg peaks of 1:4 and 1:2 DPPC/PA, the calculated unit cell parameters differ less than 1%.

Figure 5 summarizes our findings on mixed DPPC/HD and DPPC/PA monolayers at 40 mN/m. As expected, the area per hydrocarbon chain decreases with increasing molar fraction of single chain surfactant [Figs. 5(a), 5(a′)], until

TABLE II. DPPC:PA mixtures at 40mN/m at 30 °C.

Composition	In-plane Bragg peaks: Observed d-spacing (Å)	Area per chain (Å^2)	Projected area per chain (Å^2)	Unit cell (Å)	Coherence length, L (Å)	Out-of-plane Bragg rods: Tilt angle, t (degrees)	Tilt direction (degrees)
DPPC	d_{11} 4.57, d_{02} 4.31	23.27	21.00	rectangular[a] $a=5.40$, $b=8.62$	L_{11} 50, L_{02} 150	25.5°	13° from NN, non-symmetry
PA 30mN/m	d_{10} 4.20	20.37	20.28	hexagonal $a_H=4.85$	L_{10} 720	5.3°	NN[b]
3:1 DPPC:PA	d_{10} 4.35, d_{01} 4.33, d_{11} 4.25	21.43	19.97	oblique $a=4.95$, $b=4.93$ $\gamma=118.6°$	L_{10} 70, L_{01} 160, L_{11} 700	21.3°	14.9° from NN, non-symmetry
1:1 DPPC:PA	d_{10} 4.19	20.28	20.22	hexagonal $a_H=4.84$	L_{10} 490	<5.0°	NN[b]
1:2 DPPC:PA	d_{10} 4.18	20.19	20.15	hexagonal $a_H=4.83$	L_{10} 560	<5.0°	NN[b]
1:4 DPPC:PA	d_{10} 4.18	20.19	20.13	hexagonal $a_H=4.83$	L_{10} 600	<5.0°	NN[b]

[a]Small oblique distortion possible.
[b]The NN tilt direction was used to extract the listed parameters from the fitting procedure. However, with a tilt angle ⩽5°, the tilt direction is almost impossible to determine. In this case, one should think of the tilt direction as ''undetermined.''

TABLE III. DPPC:hexadecanol mixtures at 15mN/m at 30 °C.

	In-plane Bragg peaks					Out-of-plane Bragg rods	
Composition	Observed d-spacing (Å)	Area per chain (Å^2)	Projected area per chain (Å^2)	Unit cell (Å)	Coherence length, L (Å)	Tilt angle, t (degrees)	Tilt direction (degrees)
DPPC	No in-plane diffraction observed→no in-plane order						
HD	d_{10} 4.19	20.28	20.22	hexagonal $a_H=4.84$	L_{10} 850	<5.0°	NN[a]
3:1 DPPC:HD	d_{11} 4.48, d_{02} 4.27	22.49	20.33	rectangular $a=5.26$, $b=8.55$	L_{11} 90, L_{02} 580	25.3°	8.9° from NN, non-symmetry
1:1 DPPC:HD	d_{11} 4.33, d_{02} 4.25	21.35	19.96	rectangular $a=5.03$, $b=8.49$	L_{11} 95, L_{02} 590	20.8°	15.3° from NN, non-symmetry
1:2 DPPC:HD	d_{11} 4.27, d_{02} 4.23	20.87	19.86	rectangular $a=4.94$, $b=8.45$	L_{11} 210, L_{02} 560	17.9°	18.2° from NN, non-symmetry
1:4 DPPC:HD	d_{10} 4.20	20.37	20.29	hexagonal $a_H=4.85$	L_{10} 630	≤5.0°	NN[a]

[a]The NN tilt direction was used to extract the listed parameters from the fitting procedure. However, with a tilt angle ≤5°, the tilt direction is almost impossible to determine. In this case, one should think of the tilt direction as ''undetermined.''

at a molar ratio of 1:1 a minimum area per chain of about 20 Å^2 is reached. This area per chain for all mixtures is smaller than the calculated area per chain assuming ideal mixing $[A_{\text{chain}}=(\chi_{\text{DPPC}}*2*A_{\text{chain}}^{\text{DPPC}}+(1-\chi_{\text{DPPC}})*A_{\text{chain}}^{\text{PA}})/(1+\chi_{\text{DPPC}})$, where χ_{DPPC} is the mole fraction of DPPC]. The deviation from ideal mixing, meaning the difference of experimentally determined area per chain ($A_{\text{chain}}^{\text{exp}}$) and calculated area per chain ($A_{\text{chain}}^{\text{calc}}$) normalized to the experimentally determined area per chain $\Delta A/A_{\text{chain}}^{\text{exp}}=(A_{\text{chain}}^{\text{calc}}-A_{\text{chain}}^{\text{exp}})/A_{\text{chain}}^{\text{exp}}$, is largest (about 10%) at a molar ratio of 1:1 [Figs. 5(b), 5(b′)]. At this molar ratio the tilt angle is reduced to about 5° from 25° for pure DPPC [Figs. 5(c), 5(c′)]. Further increases in PA or HD do not decrease the tilt angle.

At a surface pressure of 15 mN/m, according to our isotherm and fluorescence measurements, DPPC is in the *le* phase. We did not find nor expect any Bragg peaks [Figs. 3(a), 3(a′)]. PA, on the other hand, is in a *c* phase at $\pi=15$ mN/m. For that phase we find two diffraction peaks [Fig.

TABLE IV. DPPC:hexadecanol mixtures at 40mN/m at 30 °C.

	In-plane Bragg peaks					Out-of-plane Bragg rods	
Composition	Observed d-spacing (Å)	Area per chain (Å^2)	Projected area per chain (Å^2)	Unit cell (Å)	Coherence length, L (Å)	Tilt angle, t (degrees)	Tilt direction (degrees)
DPPC	d_{11} 4.57, d_{02} 4.31	23.27	21.00	rectangular[a] $a=5.40$, $b=8.62$	L_{11} 50, L_{02} 150	25.5°	13° from NN, non-symmetry
HD	d_{10} 4.17	20.08	20.02	hexagonal $a_H=4.82$	L_{10} 620	<5.0°	NN[b]
3:1 DPPC:HD	d_{11} 4.31, d_{02} 4.24	21.24	20.07	rectangular $a=5.01$, $b=8.48$	L_{11} 110, L_{02} 700	19.1°	15.2°, from NN, non-symmetry
1:1 DPPC:HD	d_{10} 4.19	20.28	20.22	hexagonal $a_H=4.84$	L_{10} 620	<5.0°	NN[b]
1:2 DPPC:HD	d_{10} 4.18	20.15	20.10	hexagonal $a_H=4.82$	L_{10} 780	<5.0°	NN[b]

[a]Small oblique distortion possible.

[b]The NN tilt direction was used to extract the listed parameters from the fitting procedure. However, with a tilt angle ≤5°, the tilt direction is almost impossible to determine. In this case, one should think of the tilt direction as ''undetermined.''

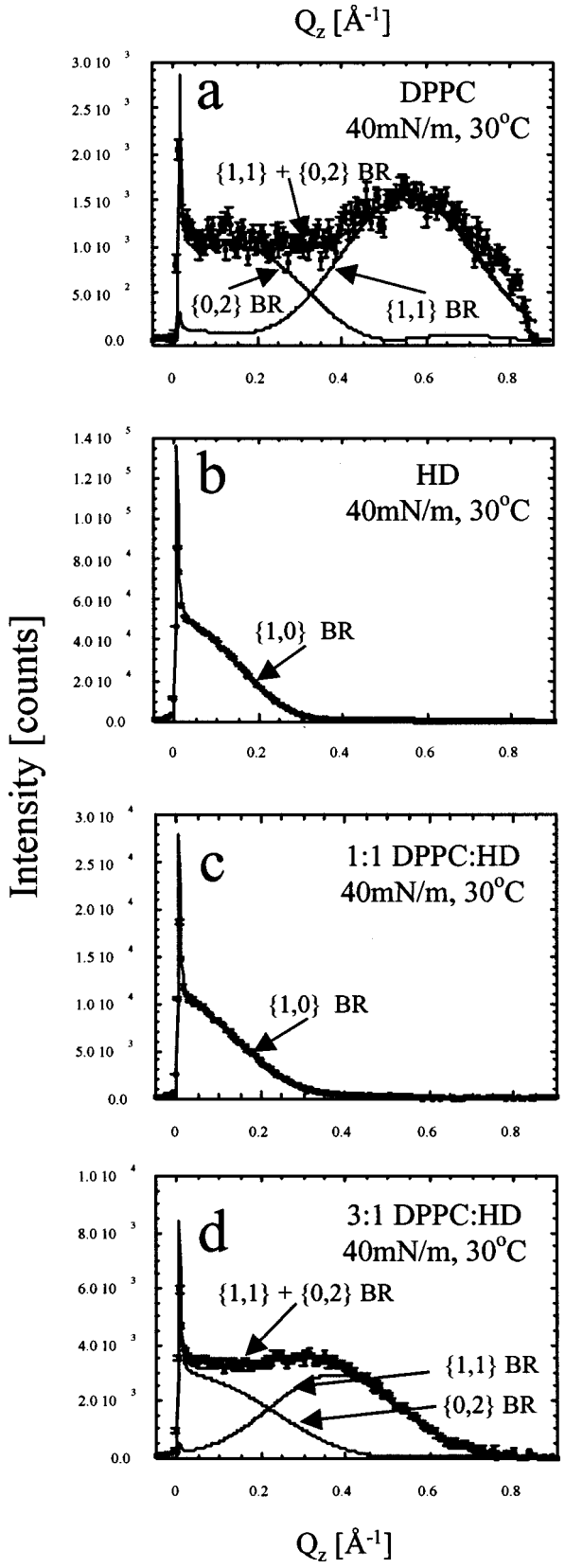

FIG. 4. Bragg rods obtained from integrating (after background subtraction) scattered intensity distribution perpendicular to the water surface over the Q_{xy} range of each Bragg peak for (a) DPPC, (b) HD, (c) 3:1 DPPC/HD, and (d) 1:1 DPPC/HD monolayers. The rods were fitted (solid line) by approximating the coherently scattering part of the phospholipid tail by a cylinder of a constant electron density. The molecular packing parameters used in the fitting procedure are listed in Table IV. All samples are at 40 mN/m and 30 °C.

3(a)] indicating a rectangular unit cell. The calculated area per chain of $A_{\text{chain}}=21.56\,\text{Å}^2$ is slightly higher than the area per chain one would expect for close packed aliphatic chains. Therefore one expects a tilt angle t of $\cos t=A_0/A_{\text{chain}}=22°$, with A_0 being the minimal area per chain reached at closest packing ($A_0=20\,\text{Å}^2$). This matches well with the tilt angle derived from Bragg rod analysis (Table I). Our data on pure PA are in good agreement with earlier studies on saturated fatty acids that show two distinct orthorhombic tilted phases under these conditions.[25] However, our results show an intermediate tilt, while for longer chain fatty acids, either a nearest neighbor (L_2) or next nearest neighbor tilt (Ov phase) is observed.[25,32]

As already mentioned, pure DPPC is 100% in the *le* phase at a pressure of 15 mN/m and shows no Bragg scattering [Fig. 3(a)]. However, fluorescence micrographs of a 3:1 mixture of DPPC/PA show *le* phase coexisting with *c* phase (see Fig. 2). As only the ordered, condensed phase contributes to the Bragg peaks, the Bragg peaks seen allow us to assign a rectangular structure with lattice parameters slightly higher than for PA to the condensed phase of the monolayer (Table I). Adding increasing amounts of PA to DPPC leads to closer rectangular packing with decreasing area per chain and decreasing tilt. Finally at a molar ratio of 1:2 DPPC/PA or higher, the packing is even more dense than for pure PA (Table I). The tilt direction remains intermediate between nearest and next nearest neighbor.

A very similar trend is observed with DPPC/HD mixtures. From our isotherm data we know that HD is likely to be in an untilted solid phase at a lateral pressure of 15 mN/m (Fig. 1). For this phase we find a single Bragg peak indicating hexagonal packing with near zero tilt [Fig. 3(a′)]. Adding HD to DPPC induces the same changes in the DPPC monolayer as described for DPPC/PA mixtures, namely a closer packing and a reduction in tilt. As in DPPC/PA mixtures, the tilt direction for all but one case remains intermediate between nearest and next nearest neighbor, and the area per chain decreases with increasing HD fraction. For the 1:4 DPPC:HD mixture, the system maintains a nearest neighbor tilt, and the area per chain is almost the same as pure HD. The results are summarized in Table III.

IV. DISCUSSION AND CONCLUSIONS

Both PA and HD form highly ordered crystalline structures with DPPC over a wide range of PA or HD fraction. This suggests that these films are good models for the solid phase fraction of natural lung surfactant monolayers, which consist mainly of DPPC with small fractions of PA.[17] These films are even better models of the solid phases of synthetic lung surfactant monolayers, which usually have higher fractions of PA or HD than the native surfactant.[13–16,40]

As is observed for bilayer systems, adding PA or HD to DPPC increases the phase transition temperature. The gel transition temperature of DPPC bilayers increases from about 42 °C (for pure DPPC) to 62 °C (for 1:2 DPPC:PA by mole) on addition of increasing fractions of palmitic acid.[41] The liquid-expanded to condensed transition is eliminated in equimolar or higher DPPC:PA monolayers at 30 °C. The *le-c* and gel to liquid crystal phase transition temperatures are

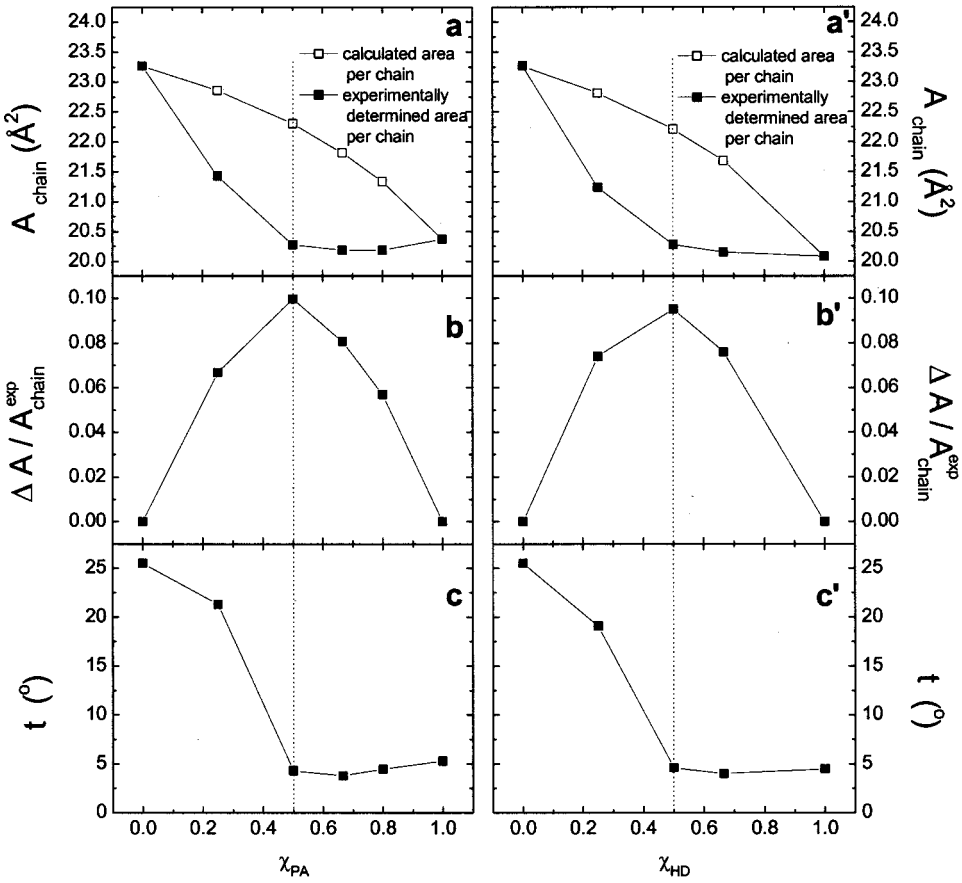

FIG. 5. Dependence of some molecular parameters on the mole fraction of PA [left panel, (a)–(c)] or HD, respectively, [right panel, (a′)–(c′)]. (a) and (a′) depict the measured area per acyl chain (filled squares) as well as the area per acyl chain calculated under the assumption of ideal mixing of DPPC and the single chain surfactant (open squares). Each DPPC counts for two acyl chains and PA or HD counts for one chain per molecule. (b) and (b′) show the deviation from ideal behavior, namely the difference of calculated and measured area per chain normalized to the measured area per chain. Variations in tilt angle of acyl chains are presented in (c) and (c′). All samples were at 40 mN/m and 30 °C.

determined by the competition between the attractive interactions between the hydrophobic aliphatic chains and the steric repulsion of the bulky phosphocholine head group. Therefore, an increased phase transition temperature can be due to better hydrophobic interaction between chains or reduced steric repulsion between heads. In the monolayer, DPPC has a minimum molecular area of about 46 Å^2 (Fig. 1),[36,42] which is limited by the relatively large head group cross sectional area. The cross sectional area of an optimally packed, all *trans*, hydrocarbon chain is about 20 Å^2,[25] so the hydrocarbon portion of the DPPC molecule would like to occupy an area of $A=2\times20\,\text{Å}^2=40\,\text{Å}^2$. This mismatch results in a tilt angle of the aliphatic chains of 25°–30° (see tables) and a reduction in the attractive interactions between the chains.[36,43] Tilting is also accompanied by a decrease in the coherence length of the crystalline packing (Tables I–IV[25]), indicative of reduced order in the lattice.

Addition of PA or HD reduces the head/tail mismatch of pure DPPC as indicated by the decrease in tilt angle of the mixed crystal. Increasing the fraction of PA or HD increases the area occupied by the chains more than the area occupied by the head groups leading to a reduction in the tilt angle of the aliphatic chains from ≈25° for pure DPPC to ≈5° at a 1:1 molar ratio of DPPC and PA or HD at 40 mN/m and 30 °C. At this composition we also find closest packing of the aliphatic chains normal to the chain axes. Further increase of the fraction of PA or HD does not change the lattice or the tilt. The coherence length of the crystalline domains also increases, indicating better order of the lattice. The enhanced order and reduced tilt lead to increased hydrophobic interactions, and are responsible for the elimination of the *le* phase at 30 °C.

This leads us to the question of what the ''perfect'' mixing ratio of DPPC and the single chain surfactants would be. From very simple geometrical considerations, assuming a cross sectional area of 20 Å^2 per aliphatic chain and 46 Å^2 per PC head in the solid state, one would expect a ratio of 3:1 DPPC/PA or DPPC/HD, respectively, if the PA or HD head took up no area. For that molar ratio the area occupied by 3 PC head groups of $A_{\text{head}}=3\times46\,\text{Å}^2=138\,\text{Å}^2$ matches the area occupied by 7 (6 from DPPC and 1 from PA or HD) aliphatic chains $A_{\text{chains}}=7\times20\,\text{Å}^2=140\,\text{Å}^2$ exactly. However, our data do not support this very simple model. For a 3:1 mixture of DPPC and single chain surfactant at 40 mN/m and 30 °C the analysis of our GIXD data reveals a mean area per chain of 21.3 Å^2 and a tilt angle of about 20° (Tables III and IV).

Instead we find closest packing, meaning a hexagonal unit cell with an area per chain of $A_{\text{chain}}\approx20\,\text{Å}^2$ and almost zero tilt angle, at 50 mol % or more of single chain surfactant (Tables II and IV and Fig. 5). The reason why our simple model fails might be that the PC headgroup is not spherical but more elliptic and the head group does not allow an orientation a 3:1 complex would require [Fig. 6(b)]. However, a more likely reason is that the HD or PA headgroup, while smaller than the projected area of the hydrocarbon chain, still occupies some area at the interface. A 1:1 ratio of PA (or HD) and DPPC seems to be sufficient to match the interfacial area

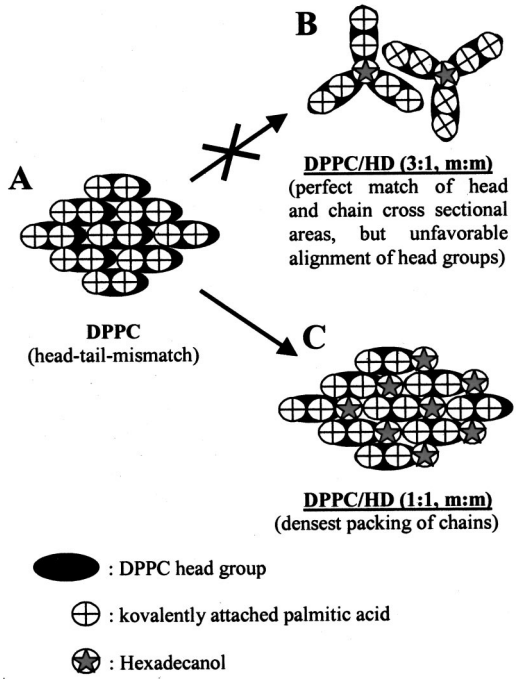

FIG. 6. Sketch of possible molecular arrangements for DPPC/HD mixtures at 40 mN/m and 30 °C.

of the headgroups and the close-packed chains [Fig. 6(c)].

Monolayer studies of phospholipids at the air–water interface in contact with simple alkanes lead to the same conclusion. In the solid state, one alkane molecule per DPPC incorporates into the monolayer whereas no alkanes incorporate into a dipalmitoylphosphoethanolamine (DPPE) monolayer.[44] For DPPE, the cross sectional area of the chains matches the headgroup cross sectional area of 40 $Å^2$ and the monolayer is untilted.[45]

It is difficult to conclude if there is a unique ratio of PA to DPPC that leads to an optimal crystal structure. The closest packing of aliphatic chains occurs at a PA or HD content of 50 mol %. From our data, we cannot conclude if further addition of PA or HD leads to the formation of mixed crystals with a higher fraction of single chain surfactant, or if we have a separation of the excess PA or HD crystals in coexistence with a 1:1 complex of PA (or HD) and DPPC. The literature data on phospholipid/fatty acid bilayers are equivocal. Based on differential thermal analysis Hui and Barton[9] find 1:1, 1:2, and 1:3 complexes of dipalmitoylphosphatidylcholine and several *n*-alcohols demixing at a ratio higher than 1:3. Eliasz *et al.*[6] report the formation of 1:2 up to 1:4 complexes of DPPC with alcohols, and demixing when the alcohol content exceeds 80%. They also report a 1:1 complex for DPPC and myristic acid. The majority of calorimetric studies find highest melting temperature for a 1:2 molar mixture of DPPC and PA.[10,41]

Some support for the formation of an excess PA or HD phase is given by the isotherms. The shape of the isotherms changes if the amount of single chain surfactant is increased over 50 mol % (Fig. 1). At molar ratios of 1:2 or 1:4 we find a kink in the isotherm indicating a second order phase transition as it is observed for pure PA or pure HD. Therefore we believe that if the amount of PA or HD exceeds 50 mol % the excess single chain surfactant is excluded from the complex with the DPPC and forms pure crystals that coexist with mixed 1:1 crystals of DPPC/PA or DPPC/HD, respectively. The deviation of ideal mixing behavior is also highest at a molar ratio of 1:1 (Fig. 5).

Addition of PA or HD to DPPC monolayers leads to a change from a tilted to untilted molecular packing, with a significantly larger correlation length, indicating a better-ordered monolayer. This correlates with the elimination of the liquid-expanded to condensed phase transition at 30 °C. Effectively, adding PA or HD is roughly equivalent to lowering the temperature of a pure DPPC monolayer. The range of concentrations of PA and HD found in natural and replacement lung surfactants makes DPPC monolayers better ordered, and effectively turns the monolayer more rigid. Similar condensation effects can be brought about by the presence of divalent ions under physiological conditions.[46] These results also suggest that PA and HD are localized in the solid phase domains of the LS monolayer. The changes induced in the solid phase of the monolayer, in turn, likely alter its collapse and respreading behavior.[22] Recent theoretical work[47,48] demonstrates that the folding transition observed in LS can be understood in terms of the mechanical property of the film. PA appears to be necessary to adjust the solid phase properties in natural lung surfactants, which helps to explain the need for PA or HD in replacement lung surfactants. As closest packing is obtained at a 1:1 molar mixture of PA (or HD) and DPPC, this suggests an upper limit to the fraction of PA necessary in a synthetic lung surfactant.

ACKNOWLEDGMENTS

The authors gratefully acknowledge beamtime at HASYLAB at DESY, Hamburg, Germany, and funding by the programs DanSync (Denmark) and TMR-Contract ERBFMGECT950059 of the European Community. K.Y.C.L. is grateful for the support from the Camille and Henry Dreyfus New Faculty Award (NF-98-048), the Searle Scholars Program/The Chicago Community Trust (99-C-105), the March of Dimes Basil O'Connor Starter Scholar Research Award (5-FY98-0728), and the American Lung Association (RG-085-N). J.A.Z. was supported by NIH Grant HL-51177 and the Tobacco Related Disease Research Program Grant 8RT-0077. The Manuel Lujan Jr., Neutron Scattering Center is a national user facility funded by the United States Department of Energy, Office of Basic Energy Sciences-Materials Science, under Contract No. W-7405-ENG-36 with the University of California. This work was also supported in part by the MRL Program of the National Science Foundation under Award Numbers DMR-9808595 (The University of Chicago) and DMR96-32716 (University of California, Santa Barbara).

[1] D. Papahadjapoulos, K. Jacobson, S. Nir, and I. Isac, Biochim. Biophys. Acta **311**, 330 (1973); L. Cruzeiro-Hansson and O. G. Mouritsen, *ibid.* **944**, 63 (1988).
[2] J. A. F. Op den Kamp, M. T. Kauertz, and L. L. M. Van Deenen, J. Biol. Chem. **261**, 169 (1986); M. Menashe, G. Romero, R. L. Biltonen, and D. Lichtenberg, *ibid.* **261**, 5328 (1986).
[3] H. Warriner, S. Idziak, N. Slack, P. Davidson, and C. Safinya, Science **271**, 969 (1996).
[4] J. T. Woodward IV and J. A. Zasadzinski, Phys. Rev. E **53**, R3044 (1996).
[5] M. Shinitzky, in *Physiology of Membrane Fluidity*, edited by M. Shinitzky (CRC Press, Boca Raton, 1984), Vol. 1, p. 1; A. R. Cossins and M. Sinensky, in *Physiology of Membrane Fluidity*, edited by M. Shinitzky (CRC Press, Boca Raton, 1984), p. 1.
[6] A. W. Eliasz, D. Chapman, and D. F. Ewing, Biochim. Biophys. Acta **448**, 220 (1976).
[7] S. Chiruvolu, H. E. Warriner, E. Naranjo, S. Idziak, J. O. Radler, R. J. Plano, J. A. Zasadzinski, and C. R. Safinya, Science **266**, 1222 (1994).
[8] S. A. Simon and T. J. McIntosh, Biochim. Biophys. Acta **773**, 169 (1984); E. S. Rowe, Biochemistry **22**, 3329 (1983).
[9] F. K. Hui and P. G. Barton, Biochim. Biophys. Acta **296**, 510 (1973).
[10] S. E. Schullery, T. A. Seder, D. A. Weinstein, and D. A. Bryant, Biochemistry **20**, 6818 (1981).
[11] J. M. Seddon, R. H. Templer, N. A. Warrender, A. Huang, G. Cevc, and D. Marsh, Biochim. Biophys. Acta **1327**, 131 (1997); A. Ortiz and J. C. Gomez-Fernandez, Chem. Phys. Lipids **45**, 75 (1987).
[12] Z. Huang and R. M. Epand, Chem. Phys. Lipids **86**, 161 (1997).
[13] D. L. Shapiro and R. H. Notter, *Surfactant Replacement Therapy* (Liss, New York, 1989).
[14] A. Cockshutt, D. Absolom, and F. Possmayer, Biochim. Biophys. Acta **1085**, 248 (1991).
[15] F. R. Poulain and J. A. Clements, West. J. Med. **162**, 43 (1995).
[16] J. Johansson and T. Curstedt, Eur. J. Biochem. **244**, 675 (1997).
[17] U. Pison, R. Herold, and S. Schürch, Colloids Surface **114**, 165 (1996).
[18] R. Veldhuizen, K. Nag, S. Orgeig, and F. Possmayer, Biochim. Biophys. Acta **1408**, 90 (1998).
[19] Y. Tanaka, T. Tsunetomo, A. Toshimitsu, K. Masuda, K. Akira, and T. Fujiwara, J. Lipid Res. **27**, 475 (1986).
[20] Y. Tanaka, T. Tsunetomo, and Y. Kanazawa, Chem. Pharm. Bull. (Tokyo) **31**, 4100 (1983).
[21] R. H. Phibbs, R. A. Ballard, J. A. Clements, D. C. Heilbron, C. S. Phibbs, M. A. Schlueter, S. H. Sniderman, W. H. Tooley, and A. Wakely, Pediatrics **88**, 1 (1991); R. Schwartz, M. Anastasia, M. Luby, J. Scanlon, and R. Kellogg, N. Engl. J. Med. **330**, 1476 (1994).
[22] M. M. Lipp, K. Y. C. Lee, D. Y. Takamoto, J. A. Zasadzinski, and A. J. Waring, Phys. Rev. Lett. **81**, 1650 (1998).
[23] M. M. Lipp, K. Y. C. Lee, A. J. Waring, and J. A. Zasadzinski, Rev. Sci. Instrum. **68**, 2574 (1997).
[24] H. M. McConnell and V. T. Moy, J. Phys. Chem. **92**, 4520 (1988).
[25] V. M. Kaganer, H. Möhwald, and P. Dutta, Rev. Mod. Phys. **71**, 779 (1999).
[26] C. M. Knobler and R. C. Desai, Annu. Rev. Phys. Chem. **43**, 207 (1992).
[27] H. McConnell, Annu. Rev. Phys. Chem. **42**, 171 (1991).
[28] J. Majewski, R. Popovitz-Biro, W. G. Bouwman, K. Kjaer, J. Als-Nielsen, M. Lahav, and L. Leiserovitz, Chem.-Eur. J. **1**, 304 (1995).
[29] J. Als-Nielsen and K. Kjaer, in *Phase Transitions in Soft Condensed Matter*, edited by T. Riste and D. Sherrington (Plenum, New York, 1989), p. 113.
[30] P. Eisenberger and W. C. Marra, Phys. Rev. Lett. **46**, 1081 (1981).
[31] J. Als-Nielsen, D. Jacquemain, K. Kjaer, F. Leveiller, M. Lahav, and L. Leiserowitz, Phys. Rep. **246**, 251 (1994).
[32] K. Y. C. Lee, J. Majewski, T. L. Kuhl, P. B. Howes, K. Kjaer, M. M. Lipp, A. J. Waring, J. A. Zasadzinski, and G. S. Smith, Biophys. J. **81**, 572 (2001).
[33] E. Teer, C. M. Knobler, C. Lautz, S. Wurlitzer, J. Kildae, and T. M. Fischer, J. Chem. Phys. **106**, 1913 (1997).
[34] C. Lautz, T. M. Fischer, M. Weygand, M. Losche, P. B. Howes, and K. Kjaer, J. Chem. Phys. **108**, 4640 (1998).
[35] K. Kjaer, J. Als-Nielsen, C. A. Helm, L. A. Laxhuber, and H. Möhwald, Phys. Rev. Lett. **58**, 2224 (1987); C. Bohm, H. Mohwald, L. Leiserovitz, J. Als-Nielsen, and K. Kjaer, Biophys. J. **64**, 553 (1993).
[36] C. A. Helm, H. Möhwald, K. Kjaer, and J. Als-Nielsen, Biophys. J. **52**, 381 (1987).
[37] G. Brezesinski, A. Dietrich, B. Struth, C. Böhm, W. G. Bouwman, K. Kjaer, and H. Möhwald, Chem. Phys. Lipids **76**, 145 (1995).
[38] M. C. Wiener, R. M. Suter, and J. F. Nagle, Biophys. J. **55**, 315 (1989).
[39] G. Brezesinski, V. M. Kaganer, H. Mohwald, and P. G. Howes, J. Chem. Phys. **109**, 2006 (1998).
[40] M. Longo, A. Bisagno, J. Zasadzinski, R. Bruni, and A. Waring, Science **261**, 453 (1993).
[41] S. Mabrey and J. Sturtevant, Biochim. Biophys. Acta **486**, 444 (1977).
[42] O. Albrecht, H. Gruler, and E. Sackmann, J. Phys. (France) **39**, 301 (1978).
[43] Y. K. Levine, Prog. Surf. Sci. **3**, 279 (1973).
[44] G. Brezesinski, M. Thoma, B. Struth, and H. Mohwald, J. Phys. Chem. **100**, 3126 (1996).
[45] C. A. Helm, P. Tippmann-Krayer, H. Mohwald, J. Als-Nielsen, and K. Kjaer, Biophys. J. **60**, 1457 (1991).
[46] M. Lipp, Thesis, University of California at Santa Barbara (1997).
[47] H. Diamant, T. A. Witten, A. Gopal, and K. Y. C. Lee, Europhys. Lett. **52**, 171 (2000).
[48] H. Diamant, T. A. Witten, C. Ege, A. Gopal, and K. Y. C. Lee, Phys. Rev. E **63**, 061602 (2001).